Numerical Methods for the One Way Water Wave Equation

Sean Carney
Advised by: Smadar Karni

Abstract

The water wave equation models incompressible, irrotational flow in unbounded domains, but its solution suffers from unnatural reflections that arise because information is not available outside of the computational domain. The one way water wave equation sidesteps this problem by using a careful boundary treatment that only allows for wave propagation in one direction. The one way equation can be framed as a conservation law whose flux integral contains an integrable singularity. Using polynomial basis functions in a finite volume computational framework, we compute flux integrals for both polynomial and wavepacket initial data. We look at various reconstruction methods on both uniform and nonuniform grids and examine error estimates and rates of convergence.

1 Introduction

Water waves are often modeled in unbounded domains. A common problem we would like to solve is the flow around a ship at sea, in which the the only meaningful interactions are those between the surface waves and the ship's body. Given by Wu [3] in 1997, the water wave equation models such flows.

1.1 Water Wave Equation (WWE)

The water wave equation models incompressible, irrotational flow in unbounded domains and is given by:

$$\frac{\partial^2 u}{\partial t^2} + \frac{\partial}{\partial x}\frac{1}{\pi} PV \int_{-\infty}^{\infty} \frac{u(y,t)}{x-y} dy = 0. \tag{1}$$

It is a linear PDE with one dimension in space and one in time, facilitating both left and right moving waves. It is also dispersive, meaning different wave numbers correspond to different speeds. Numerical solutions produced by Jennings et al. [1] are shown in the following plot

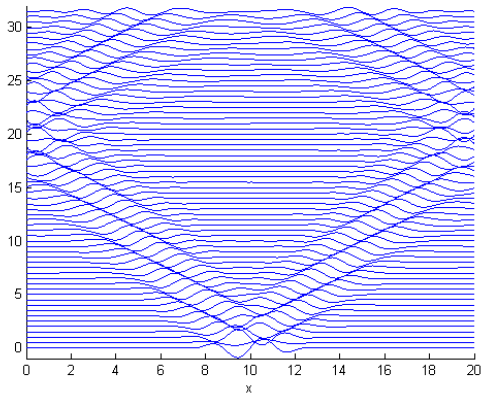

Solution to the full water wave equation over time

As the waves propagate outwards in time, around $t \approx 20$ units they hit the computational domain boundaries ($x = 0$ and $x = 20$) and reflect back in the opposite direction. This is physically incorrect, for if you were to drop a stone in the middle of a calm sea, you would expect the waves to radially propagate in all directions, but never to reflect back towards you. The problem arises when we replace the integral over the entire real number line in (1) with the bounds of the computational domain. In other words, (1) becomes

$$\frac{\partial^2 u}{\partial t^2} + \frac{\partial}{\partial x}\frac{1}{\pi} P.V. \int_0^L \frac{u(y,t)}{x-y} dy = 0. \tag{2}$$

Truncating the integral is equivalent to assuming our solution $u(x,t)$ is identically zero outside of the computational domain, which is not compatible with waves propagating in an infinite domain. Because there exists no mechanism for the waves to cleanly exit at the boundaries, they reflect backwards and interfere with the solution.

In order to deal with this problem, some analysis is performed that is beyond the scope of this paper, and afterwards we are left with the one way water wave equation.

1.2 One Way Water Wave Equation (OWWWE)

The one way equation is a linear, fractional PDE containing a half derivative in space. Like the full water wave equation, it is one dimension in time and one in space. Most importantly, it supports one way solutions to the full WWE and is given by

$$\frac{\partial u}{\partial t} \pm \frac{\partial}{\partial x}\frac{1}{\sqrt{2\pi}} \int_{-\infty}^{\infty} \frac{u(y,t)}{\sqrt{|x-y|}} dy = 0 \tag{3}$$

where the $\pm$ correspond to right and left moving waves respectively. From Jennings et al. [1] we have the following plot of the approximate solution over time:

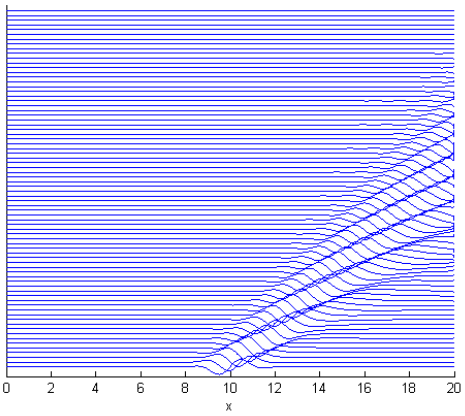

Notice the one way equation does not suffer from the same reflections at the boundaries that the full WWE does. We now turn our attention to coming up with an efficient numerical method.

The first step to solving the OWWWE numerically is to note that it can be framed as a conservation law. In particular, we have

$$u_t \pm f(u,x)_x = 0 \tag{4}$$

where the flux is given by

$$f(u,x) = \frac{1}{\sqrt{2\pi}} \int_{-\infty}^{\infty} \frac{u(y,t)}{\sqrt{|x-y|}} dy. \tag{5}$$

1.3 Finite Volume Computational Framework

Before solutions to the flux integral are discussed, we first must introduce some brief notation. In finite volume methods, we define $x_i = x_L + (i-1/2)h$ and $x_{i+1/2} = (x_i + x_{i+1})/2$, where x_L is the left endpoint of our domain. We divide our domain on $[x_L, x_R]$ into cells $I_i = [x_{i-1/2}, x_{i+1/2}]$, where i ranges from 1 to N. For this paper, we always define our domain to be on $[0, L]$. In the case of a uniform grid, we define our constant step size $h = 1/N$. If we integrate (4) over cell I_i and divide by h, we obtain the semi-discrete form of our conservation law

$$\frac{d}{dt}\overline{u}_i(t) = -\frac{1}{h}(f_{i+1/2} - f_{i-1/2}). \tag{6}$$

It is often the case in finite volume methods that we compute numerical approximations of the solution's cell averages, and the $\overline{u}_i$ term in (6) reflects this. The flux at the cell

interface is

$$f_{i\pm1/2} = \frac{1}{\sqrt{2\pi}} \int_{-\infty}^{\infty} \frac{u(y,t)}{\sqrt{|x_{i\pm1/2} - y|}} dy \tag{7}$$

where the $\pm$ correspond to the flux at the right and left endpoint of cell I_i respectively. We can also re-write (7) as

$$f_{i\pm1/2} = \frac{1}{\sqrt{2\pi}} \sum_j \int_{I_j} \frac{u(y,t)}{\sqrt{|x_{i\pm1/2} - y|}} dy \tag{8}$$

where j sums over all integers.

1.4 Polynomial Approximations

In order to solve (8), we approximate our solution function $u(x,t)$ with piecewise polynomials over each cell I_j. When $u(x,t)$ is replaced by its polynomial approximation $P_j(x,t)$, we can integrate over the singularity in (8) exactly. The final approximation comes when we truncate the summation of integrations at the boundary of the computational domain. It is important to note that although this truncation of the domain will result in errors at the boundaries, the one way equation does not allow for these errors to reflect back and interfere with the solution. We are left then with

$$F_{i\pm1/2} = \frac{1}{\sqrt{2\pi}} \sum_{j=1}^{N} \int_{I_j} \frac{P_j(y,t)}{\sqrt{|x_{i\pm1/2} - y|}} dy \tag{9}$$

where $F_{i+1/2}$ denotes the approximation to $f_{i+1/2}$. So, in order to solve the OWWWE, we compute the numerical flux $F_{i+1/2}$ for each grid point in the domain and then integrate (6) in time with an appropriate order Runge-Kutta solver.

How do we choose and construct our approximating polynomial $P_j(x,t)$? As previously mentioned for finite volume methods, when we solve the PDE we are actually computing numerical approximations of the solution's cell averages. We approximate solutions locally by polynomials that are constructed with those averages. In the case of linear reconstruction, for example, we want our polynomial to be such that

$$\frac{1}{h} \int_{I_{j-1}} P_j(y,t) dy = \overline{u}_{j-1} \qquad \frac{1}{h} \int_{I_j} P_j(y,t) dy = \overline{u}_j. \tag{10}$$

Since a linear polynomial contains two coefficients, and we have supplied two conditions in (10) that it must satisfy, there is one unique answer $P_j(x,t)$. We choose, however, to express $P_j(x,t)$ in terms of linear basis functions so that

$$P_j(x,t) = \overline{u}_{j-1} \varphi_j^{-1}(x,t) + \overline{u}_j \varphi_j^0(x,t)$$

where the basis functions φ_j^{-1} and φ_j^0 satisfy the following properties:

$$\int_{I_{j-1}} \varphi_j^0 dy = 0 \qquad \int_{I_j} \varphi_j^0 dy = h \qquad \int_{I_j} \varphi_j^{-1} dy = 0 \qquad \int_{I_{j-1}} \varphi_j^{-1} dy = h. \tag{11}$$

It turns out that the summation in (9) can be cast as matrix multiplication, and decomposing $P_j(x,t)$ into basis functions allows us to gain insight into the entries and structure of the coefficient matrix.

2 Flux Integration on Uniform Grids

We are interested in computing flux integrals on grids with a constant step size for various types of initial data $u(x, t = 0)$. We reconstruct both polynomial and wavepacket initial data using first, second, and third order polynomial approximations.

2.1 First Order Polynomial Reconstruction

As mentioned above, for linear reconstruction our polynomial is

$$P_j = \bar{u}_{j-1}\varphi_j^{-1} + \bar{u}_j\varphi_j^0$$

Our flux then becomes

$$F_{i+1/2} = \frac{1}{\sqrt{2\pi}} \sum_{j=1}^{N} \int_{I_j} \frac{\bar{u}_{j-1}\varphi_j^{-1} + \bar{u}_j\varphi_j^0}{\sqrt{|x_{i+1/2} - y|}} dy$$

$$F_{i+1/2} = \frac{1}{\sqrt{2\pi}} \sum_{j=0}^{N} \bar{u}_j \left(\int_{I_{j+1}} \frac{\varphi_{j+1}^{-1}}{\sqrt{|x_{i+1/2} - y|}} dy + \int_{I_j} \frac{\varphi_j^0}{\sqrt{|x_{i+1/2} - y|}} dy \right)$$

Note that when $j = 0$, we only count the contribution from the integral over I_{j+1}. Likewise, when $j = N$, we only count the contribution from the integral over I_j. We now derive our basis functions, insert them in our flux, and transform the expressions into a form well suited for integration. Firstly, for φ_j^0, we have

$$h = A \int_{I_j} \varphi_j^0 dy$$

$$h = A \int_{x_{j-1/2}}^{x_{j+1/2}} (y - x_{j-1}) dy = \frac{A}{2} \left(\left(x_{j+1/2} - x_{j-1}\right)^2 - \left(x_{j-1/2} - x_{j-1}\right)^2 \right)$$

$$h = \frac{A}{2} \left(\left(\frac{3}{2}h\right)^2 - \left(\frac{1}{2}h\right)^2 \right) = \frac{A}{2} \left(2h^2\right)$$

$$\Rightarrow A = \frac{1}{h}.$$

Similarly for φ_j^{-1}

$$h = B \int_{I_{j-1}} \varphi_j^{-1} dy$$

$$h = B \int_{x_{j-3/2}}^{x_{j-1/2}} (y - x_j) dy = \frac{B}{2} \left(\left(x_{j-1/2} - x_j \right)^2 - \left(x_{j-3/2} - x_j \right)^2 \right)$$

$$h = \frac{B}{2} \left(\left(-\frac{1}{2} h \right)^2 - \left(-\frac{3}{2} h \right)^2 \right) = \frac{B}{2} \left(-2h^2 \right)$$

$$\Rightarrow B = -\frac{1}{h}.$$

Collecting all the terms, we can now write the flux integral as:

$$F_{i+1/2} = \frac{1}{\sqrt{2\pi}} \sum_{j=0}^{N} \frac{\bar{u}_j}{h} \left(\int_{x_{j+1/2}}^{x_{j+3/2}} \frac{-(y - x_{j+1})}{\sqrt{|x_{i+1/2} - y|}} dy + \int_{x_{j-1/2}}^{x_{j+1/2}} \frac{y - x_{j-1}}{\sqrt{|x_{i+1/2} - y|}} dy \right)$$

Now let $z = y - x_j$, then $y - x_{j-1} = y - (x_j - h) = z + h$ and $y - x_{j+1} = y - (x_j + h) = z - h$. The expression in the denominator becomes $x_{i+1/2} - x_j - z = (i - j + 1/2)h - z$. So

$$F_{i+1/2} = \frac{1}{\sqrt{2\pi}} \sum_{j} \frac{\bar{u}_j}{h} \left(\int_{h/2}^{3h/2} \frac{-(z - h)}{\sqrt{|(i - j + 1/2)h - z|}} dz + \int_{-h/2}^{h/2} \frac{z + h}{\sqrt{|(i - j + 1/2)h - z|}} dz \right).$$

If we distribute the $1/h$ term in the numerators and retrieve a factor of $1/\sqrt{h}$ from the denominators, we can write:

$$F_{i+1/2} = \frac{1}{\sqrt{2\pi}} \sum_{j} \frac{\bar{u}_j}{\sqrt{h}} \left(\int_{h/2}^{3h/2} \frac{-(z/h - 1)}{\sqrt{|(i - j + 1/2) - z/h|}} dz + \int_{-h/2}^{h/2} \frac{z/h + 1}{\sqrt{|(i - j + 1/2) - z/h|}} dz \right).$$

Finally, let $w = z/h$ implying $dz = h\, dw$ to end up with

$$F_{i+1/2} = \frac{\sqrt{h}}{\sqrt{2\pi}} \cdot \sum_{j} \bar{u}_j \left(\int_{1/2}^{3/2} \frac{-(w - 1)}{\sqrt{|(i - j + 1/2) - w|}} dw + \int_{-1/2}^{1/2} \frac{w + 1}{\sqrt{|(i - j + 1/2) - w|}} \right). \tag{12}$$

In summary, after our scaling and shifting our integrals, we have that:

$$\varphi_j^{-1} = -w \qquad \varphi_j^0 = w + 1$$

or

$$\varphi_{j+1}^{-1} = -(w - 1) \qquad \varphi_j^0 = w + 1.$$

In general, for any reconstruction method, we can always shift and scale our integrals so that they are over unit intervals and so that the expression in the square root in the

denominators is $|(i-j+1/2)-w|$. This greatly simplifies the process of finding our basis functions.

For example, the conditions (11) we stated previously for first order reconstruction would become

$$\int_{-3/2}^{1/2} \varphi_j^0 dy = 0 \qquad \int_{-1/2}^{1/2} \varphi_j^0 dy = 1 \qquad \int_{-1/2}^{1/2} \varphi_j^{-1} dy = 0 \qquad \int_{-3/2}^{1/2} \varphi_j^{-1} dy = 1.$$

We use this to our advantage when we are solving for basis functions for higher order reconstruction efforts.

So, in order to solve for the flux at cell interface $x_{i+1/2}$, we simply evaluate the integrals in (12) exactly and sum for the appropriate values of $i-j$. It is important to note that for linear reconstruction of first order polynomial data, the flux should be *exact*, with no error. In general, order n reconstruction of order n polynomial data should be exact. This was always the first step in verifying a correct implementation of the numerical method. We now briefly summarize the way in which we generate error estimates before stating results.

2.2 Error Estimations

In estimating error, there are two cases to consider. The first is when the exact value of the quantity in question is known. The second is when it is not. The exact value of the flux over our computational domain is given by

$$f(u,x) = \frac{1}{\sqrt{2\pi}} \int_0^L \frac{u(y)}{\sqrt{|x-y|}} dy. \tag{13}$$

Since we only consider flux integrals for initial data, we can write $u(x,t)$ simply as $u(x)$ from here on out. We consider two types of initial data $u(x)$–polynomial data, for which (13) is known, and wavepacket data, for which (13) is not. In the case of the former, our error is simply

$$e^N = \left| f - F^N \right|$$

where f is the exact value, and F^N denotes the approximate value when we divide the domain into N intervals. In the latter, we compare subsequent estimates to f to get

$$e^N = \left| F^{2N} - F^N \right|.$$

When we double the number of grid points N, we also have twice as many flux estimates, so care must be taken to compare estimates only on grid points that overlap. We are also interested in two different norms, the L_∞ and the L_1 norm. Given an array of error values across the domain, the L_∞ norm is

$$||e||_\infty = \max_i |e_i|$$

and the L_1 norm is

$$||e||_1 = he_1 + he_2 + \ldots + he_N = h\sum_{i=1}^{N} |e_i| \,.$$

Intuitively, $||e||_\infty$ gives an upper bound on the error, while $||e||_1$ gives a sense of the average error across the domain. Not only are we interested in the magnitudes of the errors themselves, but also how quickly they decrease upon mesh refinement, which is doubling the number of sampling points N, or halving step size h. Given in Runborg [2], we have that the rate of convergence of our error estimates is

$$p = \log_2 \left(\frac{e^N}{e^{2N}} \right).$$

For example, if $p = 2$, then halving our step size implies our error should decrease by $(1/2)^2 = 1/4$. Equipped with these definitions, we can now examine the results from our reconstruction methods of various initial data.

2.3 Linear Reconstruction Results

As previously mentioned, we expect that linear reconstruction of linear initial data should give exact answers. The following table confirms this expectation. All of the calculations in this paper were performed on a grid from $[0, 1]$ broken into N cells.

N	$\|\|error\|\|_\infty$	$\|\|error\|\|_1$
20	1.11022302463e-15	3.9135361618e-16
40	2.3037127761e-15	6.51258560969e-16
80	2.33146835171e-15	7.7641885976e-16
160	4.88498130835e-15	1.17757366358e-15
320	6.43929354283e-15	1.49482138364e-15
640	9.14546216535e-15	2.16233620094e-15
1280	1.33781874467e-14	3.18952255286e-15
2560	2.0872192863e-14	4.66362672823e-15
5120	3.12250225676e-14	5.81503675638e-15

Linear Reconstruction – Linear Data: $u(x, t = 0) = 3x - 2$

Since the error norms are close to machine precision, we conclude the method is exact.

While these results establish the correctness of our integral formulas, they do not tell us anything about the order of our method. So, starting now and throughout the rest of

the section, we will only be considering fifth order polynomial $u(x) = -5x^5 + 5x^4$ and wavepacket initial data. The wavepacket is piecewise continuous and is defined as:

$$u(x) = \begin{cases} 0 & x < 0.35 \\ \cos^6\left(10\pi/3(x-1/2)\right)\sin\left(50\pi/3(x-1/2)\right) & x \in [0.35, 0.65] \\ 0 & x > 0.65 \end{cases}$$

The results for linear reconstruction are as follows:

N	$\|\|error\|\|_\infty$	$rate_{L\infty}$	$\|\|error\|\|_1$	$rate_{L1}$
20	0.000678679488803	1.54511725659	0.000168122550086	2.35031289375
40	0.00023256164087	2.1055155485	3.29694185941e-05	2.3112354907
80	5.40399261139e-05	2.30058670677	6.64293616018e-06	2.36708397229
160	1.09690531337e-05	2.38976385867	1.28764694233e-06	2.41686244011
320	2.09304485788e-06	2.43548089405	2.41128592452e-07	2.44927198023
640	3.8692405735e-07	2.46058904013	4.41513896545e-08	2.46879442376
1280	7.02934121466e-08	2.47509436268	7.97559702624e-09	2.48043775906
2560	1.26426169533e-08	2.48383133488	1.42914743739e-09	2.4874690383
5120	2.2601082672e-09	2.48927417234	2.54843899071e-10	2.49180704477
10240	4.02515909492e-10	2.49256421512	4.5307028268e-11	2.49455767119
20480	7.15231207593e-11	2.49601015104	8.03949727564e-12	2.49634254434
40960	1.26786359189e-11		1.42480328276e-12	

Linear Reconstruction: $u(x, t = 0) = -5x^5 + 5x^4$

N	$\|\|error\|\|_\infty$	$rate_{L\infty}$	$\|\|error\|\|_1$	$rate_{L1}$
20	0.0755013715397	0.75594116595	0.00484061363617	1.23151991426
40	0.0447088887059	2.51334992519	0.00206146509393	2.82636138453
80	0.00783069228031	2.9621238621	0.000290640699512	2.94056358505
160	0.00100487496059	2.86236497604	3.78580801944e-05	2.86554056695
320	0.00013818290174	2.74645623881	5.19451401576e-06	2.73707975962
640	2.0591529133e-05	2.64438328479	7.79115445823e-07	2.6321394007
1280	3.29344116815e-06	2.57732102844	1.25675002305e-07	2.56693481827
2560	5.51821950412e-07	2.53979296693	2.12092115833e-08	2.53276650079
5120	9.48953880475e-08	2.5207746379	3.66510006165e-09	2.51584363439
10240	1.65354617776e-08	2.51112727015	6.40827938358e-10	2.50767226792
20480	2.9006257396e-09		1.12682601665e-10	

Linear Reconstruction: $u(x, t = 0) = \cos^6\left(10\pi/3(x-1/2)\right)\sin\left(50\pi/3(x-1/2)\right)$

We see that the results for linear reconstruction seem to be converging at a rate of $p \approx 2.5$. We now move on to results from higher order reconstruction methods.

2.4 Quadratic Reconstruction – Upwind Stencil

For quadratic polynomial reconstruction, we specify three conditions that the cell averages must satisfy. When we use an upwind stencil, we take information in the direction of propagation–in this case from the left to the right. Our polynomial expression for upwind quadratic reconstruction in terms of its basis functions is

$$P_j(x) = \overline{u}_{j-2}\varphi_j^{-2} + \overline{u}_{j-1}\varphi_j^{-1} + \overline{u}_j\varphi_j^0.$$

The corresponding flux integrals become

$$F_{i+1/2} = \frac{1}{\sqrt{2\pi}} \sum_{j=-1}^{N} \overline{u}_j \left(\int_{I_{j+2}} \frac{\varphi_{j+2}^{-2}}{\sqrt{|x_{i+1/2} - y|}} dy + \int_{I_{j+1}} \frac{\varphi_{j+1}^{-1}}{\sqrt{|x_{i+1/2} - y|}} dy + \int_{I_j} \frac{\varphi_j^0}{\sqrt{|x_{i+1/2} - y|}} dy \right).$$

Care must be taken to include the proper integrals at the extreme values of j. As a general rule for all reconstruction stencils, as we sum over all the values of j, we only count the contribution from basis function φ_k^m when $k + j \in [1, N]$. The flux estimation results of quintic and wavepacket initial data are

N	$\|\|error\|\|_\infty$	$rate_{L\infty}$	$\|\|error\|\|_1$	$rate_{L1}$
20	0.000245601482888	3.05906994211	5.06308230147e-05	3.15435481845
40	2.94685775708e-05	3.28637529111	5.68669020404e-06	3.30515308117
80	3.02038033217e-06	3.38642870849	5.75319841297e-07	3.39199326247
160	2.88831804918e-07	3.43602073929	5.48046785618e-08	3.43938034396
320	2.66869969456e-08	3.46232933558	5.05197258159e-09	3.46521911213
640	2.42122261129e-09	3.47695800158	4.57431523736e-10	3.47949844864
1280	2.17453333118e-10	3.48501491794	4.10102755791e-11	3.48758824986
2560	1.94210203475e-11	3.49759329382	3.65615005719e-12	3.49254636612
5120	1.71945790939e-12	3.48731905766	3.24834983131e-13	3.49771368645
10240	1.53321799701e-13		2.87571642931e-14	

Quadratic Upwind: $u(x, t = 0) = -5x^5 + 5x^4$

N	$\|\|error\|\|_\infty$	$rate_{L\infty}$	$\|\|error\|\|_1$	$rate_{L1}$
20	0.21115471372	1.97826801586	0.0132837467972	2.4397843278
40	0.0535898780333	3.31809636619	0.00244834335598	3.49999465407
80	0.0053732399355	3.76683610643	0.000216405825605	3.81694495469
160	0.00039473494672	3.67975812332	1.53551486304e-05	3.72979640578
320	3.08026446141e-05	3.6216147809	1.15737321873e-06	3.62736355158
640	2.50249560492e-06	3.56182315131	9.36544018574e-08	3.56431488172
1280	2.11913056547e-07	3.52928099517	7.9170338372e-09	3.53009218944
2560	1.83543188911e-08	3.5138732047	6.85328613472e-10	3.51422970054
5120	1.60678229402e-09	3.50657976779	5.99805319551e-11	3.5067396587
10240	1.41374585649e-10	3.50288036783	5.27687113905e-12	3.5031373982
20480	1.24709426813e-11		4.65400722397e-13	

Quadratic Upwind: $u(x, t = 0) = \cos^6(10\pi/3(x - 1/2)) \sin(50\pi/3(x - 1/2))$

2.5 Quadratic Reconstruction – Centered Stencil

For quadratic reconstruction using a centered stencil, three conditions on cell averages must be satisfied, and we take information both upwind and downwind from the direction of propagation. In terms of its basis functions, our polynomial is

$$P_j(x) = \overline{u}_{j-1}\varphi_j^{-1} + \overline{u}_j\varphi_j^0 + \overline{u}_{j+1}\varphi_j^{+1}.$$

and so the corresponding flux integrals become

$$F_{i+1/2} = \frac{1}{\sqrt{2\pi}} \sum_{j=0}^{N+1} \overline{u}_j \left(\int_{I_{j+1}} \frac{\varphi_{j+1}^{-1}}{\sqrt{|x_{i+1/2} - y|}} dy + \int_{I_j} \frac{\varphi_j^0}{\sqrt{|x_{i+1/2} - y|}} dy + \int_{I_{j-1}} \frac{\varphi_{j-1}^{+1}}{\sqrt{|x_{i+1/2} - y|}} dy \right).$$

The reconstruction results of quintic polynomial and wavepacket initial data are as follows:

N	$\|\|error\|\|_\infty$	$rate_{L\infty}$	$\|\|error\|\|_1$	$rate_{L1}$
20	4.16809329311e-05	4.10481468173	2.17491679778e-05	4.04499526582
40	2.42250724869e-06	2.90755463408	1.3175822641e-06	4.01161649627
80	3.22852330981e-07	3.14081761205	8.16884853819e-08	4.0027742444
160	3.66035842747e-08	3.30801634502	5.09572204085e-09	3.99822957985
320	3.69582559001e-09	3.38672430383	3.18873697152e-10	3.99705990015
640	3.53350626536e-10	3.42929922657	1.99702624663e-11	3.9971398129
1280	3.28007621064e-11	3.45578119658	1.25061833719e-12	3.99822344625
2560	2.98944202726e-12	3.45994070898	7.82599571085e-14	3.95338107568
5120	2.71671574126e-13		5.05188339078e-15	

Quadratic Centered: $u(x, t = 0) = -5x^5 + 5x^4$

N	$\|\|error\|\|_\infty$	$rate_{L\infty}$	$\|\|error\|\|_1$	$rate_{L1}$
20	0.0195869165471	-0.501732475733	0.00140942428601	0.151978201571
40	0.0277333669469	3.6600442537	0.00126850374365	3.72650593258
80	0.00219391345752	3.85098705512	9.58300442174e-05	3.95530309558
160	0.000152039655058	4.09491285761	6.17784225489e-06	4.07909285725
320	8.89744425792e-06	4.09022007813	3.65516940352e-07	4.08799592284
640	5.22379762335e-07	4.06982881905	2.14930532547e-08	4.07292897181
1280	3.11061163216e-08	4.05432610853	1.27709829193e-09	4.05480416756
2560	1.87228527126e-09	4.03975289437	7.68434125149e-11	4.04034344769
5120	1.1383746723e-10	4.02692212329	4.6702708969e-12	4.0292647013
10240	6.98330282489e-12	3.98475931857	2.86030626128e-13	4.01840774136
20480	4.41091607684e-13		1.765026669e-14	

Quadratic Centered: $u(x, t = 0) = \cos^6(10\pi/3(x - 1/2)) \sin(50\pi/3(x - 1/2))$

2.6 Cubic Reconstruction – Slight Upwind

For cubic reconstruction on a slightly upwinded stencil, four conditions on cell averages must be satisfied. We take information both upwind and downwind from the direction of propagation, but give a bias in the upwind direction. In terms of its basis functions, our polynomial is

$$P_j(x) = \overline{u}_{j-2}\varphi_j^{-2} + \overline{u}_{j-1}\varphi_j^{-1} + \overline{u}_j\varphi_j^0 + \bar{u}_{j+1}\varphi_j^{+1}$$

where the flux is given by

$$F_{i+1/2} = \frac{1}{\sqrt{2\pi}} \sum_{j=-1}^{N+1} \overline{u}_j \left(\int_{I_{j+2}} \frac{\varphi_{j+2}^{-2}}{\sqrt{|x_{i+1/2} - y|}} dy + \int_{I_{j+1}} \frac{\varphi_{j+1}^{-1}}{\sqrt{|x_{i+1/2} - y|}} dy \right.$$
$$\left. + \int_{I_j} \frac{\varphi_j^0}{\sqrt{|x_{i+1/2} - y|}} dy + \int_{I_{j-1}} \frac{\varphi_{j-1}^{+1}}{\sqrt{|x_{i+1/2} - y|}} dy \right).$$

The reconstruction results for quintic polynomial and wavepacket initial data are as follows:

N	$\|\|error\|\|_\infty$	$rate_{L\infty}$	$\|\|error\|\|_1$	$rate_{L1}$
20	5.59662051824e-06	4.15440624012	1.83961851888e-06	4.57126479737
40	3.14285950986e-07	4.32362202393	7.73820000861e-08	4.48235015483
80	1.56958575581e-08	4.40000352519	3.46192857159e-09	4.46049342226
160	7.43450412344e-10	4.43970793849	1.57244617154e-10	4.46314012271
320	3.42583739155e-11	4.46082087873	7.129133308e-12	4.47112065603
640	1.55570001326e-12	4.52531329987	3.21436583947e-13	4.46884055922
1280	6.75570710484e-14		1.45157757342e-14	

Cubic Slight Upwind: $u(x, t = 0) = -5x^5 + 5x^4$

N	$\|\|error\|\|_\infty$	$rate_{L\infty}$	$\|\|error\|\|_1$	$rate_{L1}$
20	0.0815670491826	1.85630381287	0.0046267633856	1.91620757365
40	0.0225274286353	4.08742495361	0.00122586129367	4.43813565119
80	0.00132517766187	4.87215937023	5.65495790811e-05	4.9421979447
160	4.52488965019e-05	4.99036711837	1.83941426756e-06	4.98637225623
320	1.4235010781e-06	4.9136833137	5.80272423781e-08	4.91300350576
640	4.72271495244e-08	4.79684970421	1.92606308711e-09	4.79220825191
1280	1.69901059888e-09	4.6861011583	6.95139678658e-11	4.67960758637
2560	6.59992616114e-11	4.60151242622	2.71250050283e-12	4.5983765397
5120	2.7186031204e-12	4.34012988471	1.11974867588e-13	4.54217104378
10240	1.34225963677e-13		4.80607814449e-15	

Cubic Slight Upwind: $u(x, t = 0) = \cos^6(10\pi/3(x - 1/2)) \sin(50\pi/3(x - 1/2))$

Lastly, we examine fourth order polynomial reconstruction.

2.7 Quartic Reconstruction – Centered

For quartic reconstruction on a centered stencil, five different conditions on cell averages must be satisfied, and we take information both upwind and downwind from the direction of propagation. In terms of its basis functions, our polynomial is

$$P_j(x) = \overline{u}_{j-2}\varphi_j^{-2} + \overline{u}_{j-1}\varphi_j^{-1} + \overline{u}_j\varphi_j^0 + \overline{u}_{j+1}\varphi_j^{+1} + \overline{u}_{j+2}\varphi_j^{+2}$$

where the flux is given by

$$F_{i+1/2} = \frac{1}{\sqrt{2\pi}} \sum_{j=-1}^{N+1} \overline{u}_j \left(\int_{I_{j+2}} \frac{\varphi_{j+2}^{-2}}{\sqrt{|x_{i+1/2} - y|}} dy + \int_{I_{j+1}} \frac{\varphi_{j+1}^{-1}}{\sqrt{|x_{i+1/2} - y|}} dy \right.$$
$$\left. + \int_{I_j} \frac{\varphi_j^0}{\sqrt{|x_{i+1/2} - y|}} dy + \int_{I_{j-1}} \frac{\varphi_{j-1}^{+1}}{\sqrt{|x_{i+1/2} - y|}} dy + \int_{I_{j-2}} \frac{\varphi_{j-2}^{+2}}{\sqrt{|x_{i+1/2} - y|}} dy \right).$$

The reconstruction results for quintic polynomial and wavepacket initial data are as follows:

N	$\|\|error\|\|_\infty$	$rate_{L\infty}$	$\|\|error\|\|_1$	$rate_{L1}$
20	1.00537837777e-07	5.37402999648	3.0968962797e-08	5.78403618566
40	2.42429415431e-09	5.41936574098	5.62028414086e-10	5.85942284245
80	5.66491853426e-11	5.44628620091	9.68046545702e-12	5.90648279857
160	1.29926625014e-12	5.44309760195	1.61386702613e-13	5.96799538511
320	2.98649993624e-14		2.57823276617e-15	

Quartic Centered: $u(x, t = 0) = -5x^5 + 5x^4$

N	$\|\|error\|\|_\infty$	$rate_{L\infty}$	$\|\|error\|\|_1$	$rate_{L1}$
20	0.0377571760034	1.19322580172	0.00315765791132	1.88255481596
40	0.0165121165901	5.00654121849	0.00085636638253	5.13163510098
80	0.000513669364748	5.81374215421	2.44277528943e-05	5.8861762004
160	9.13214691561e-06	6.05081331932	4.13016994502e-07	6.06837611715
320	1.3775157795e-07	6.08518068409	6.15466877891e-09	6.08600209689
640	2.02896552337e-09	6.07469443659	9.06015235823e-11	6.07674531395
1280	3.01029756677e-11	6.03546163505	1.34231018491e-12	6.05910390843
2560	4.58938442804e-13		2.01317191074e-14	

Quartic Centered: $u(x, t = 0) = \cos^6(10\pi/3(x - 1/2)) \sin(50\pi/3(x - 1/2))$

2.8 Comments on Rate of Convergence

For linear reconstruction, we saw that the rate of convergence was approaching $p = 2.5$ as we continually refined our mesh. In general, it is apparent that for a polynomial reconstruction method of degree r, we seem to get $p \approx r + 1.5$ for the rate of convergence. There are a couple of exceptions to this rule, namely for second and fourth order centered stencils, in which we get $p = r + 2$. This result can be explained by the symmetry of the stencil, for some of the error terms in the Taylor expansions cancel one another out. We are not able to explain, however, the $p \approx r + 1.5$ results that we see in general. It can be shown analytically that the rate of convergence p is *at least* one integer higher than the order of polynomial reconstruction, so our results do not violate this inequality. We are, however, currently unable to explain this extra half-order, although it is a good problem to have indeed.

3 Flux Integration on Nonuniform Grids

All of the calculations so far have been done under the assumption that step size is constant throughout the computational domain. Grids in which step size is variable, however, are of both practical and theoretical interest. Practically, grids with nonconstant step size allow for both more accurate and more efficient solutions. The idea is simple. When the numerical solution is more complicated and requires more attention, step size is reduced to provide more accuracy. On the other hand, when the solution is changing slowly or not at all, we can increase our step size to speed up our calculation while not worrying about a major loss of accuracy.

Theoretically, we are interested to see if the computational stencils that converge for the uniform case still converge for the nonuniform case, and furthermore, if they maintain their high orders of accuracy. After observing the extra half-order of convergence in the uniform cases, we were particularly interested to see if these higher convergence rates were still valid for nonuniform grids.

In the following calculations, we consider an expanding grid. Consider a function f from our analytic variable to the discrete sampling variable. In the case of a uniform mesh, our function f was simply $f(y) = y$. This implies that the step sizes, described by the rate of change of f, were constant. For the expanding grid, we chose $f(y) = y^2$, which means that the step sizes were increasing linearly throughout the domain.

3.1 Derivation of First Order Linear Method

We still wish to express our polynomials as linear combinations of basis functions based on cell averages. So for first order reconstruction, we still have

$$P_j(x) = \overline{u}_{j-1}\varphi_j^{-1} + \overline{u}_j\varphi_j^0.$$

The conditions for the basis functions, however, become

$$\int_{I_{j-1}} \varphi_j^0 dy = 0 \qquad \int_{I_j} \varphi_j^0 dy = h_j \qquad \int_{I_j} \varphi_j^{-1} dy = 0 \qquad \int_{I_{j-1}} \varphi_j^{-1} dy = h_{j-1} \quad (14)$$

where we note the subscripts on the step size h. The basis functions then become

$$\varphi_j^{-1}(y) = \frac{-2}{h_j + h_{j-1}}(y - x_j) \qquad \varphi_j^0(y) = \frac{2}{h_j + h_{j-1}}(y - x_{j-1})$$

where we omit their derivation in the interest of space. Note that if we let $h_{j-1} = h_j = h$, the basis functions reduce to their form for the uniform mesh case. For notation, we will use $\mu_j = (h_j + h_{j-1})/2$ so that

$$\varphi_j^{-1}(y) = \frac{-1}{\mu_j}(y - x_j) \qquad \varphi_j^0(y) = \frac{1}{\mu_j}(y - x_{j-1}). \quad (15)$$

Inserting our basis functions into the expression for the numerical flux, we have

$$F_{i+1/2} = \frac{1}{\sqrt{2\pi}} \sum_{j=1}^{N} \bar{u}_j \left(\int_{I_j} \frac{(1/\mu_j)(y - x_{j-1})}{\sqrt{|x_{i+1/2} - y|}} dy + \int_{I_{j+1}} \frac{(-1/\mu_{j+1})(y - x_{j+1})}{\sqrt{|x_{i+1/2} - y|}} dy \right).$$

To make the discussion easier, we will refer to the integral over I_j as integral (A) and the integral over I_{j+1} as integral (B)

Integral (A)

Let $z = y - x_j$, which means $y = z + x_j$ and $dz = dy$. The upper bound of the integral becomes $x_{j+1/2} - x_j = h_j/2$ and the lower bound becomes $x_{j-1/2} - x_j = -h_j/2$. The expression

$$y - x_{j-1} = z + x_j - x_{j-1} = z + (h_j + h_{j-1})/2 = z + \mu_j.$$

So, the integral can be written:

$$\int_{-h_j/2}^{h_j/2} \frac{(1/\mu_j)(z + \mu_j)}{\sqrt{|x_{i+1/2} - z - x_j|}} dz = \int_{-h_j/2}^{h_j/2} \frac{z/\mu_j + 1}{\sqrt{|x_{i+1/2} - z - x_j|}} dz.$$

In general, what is $x_{i+1/2} - x_j$?

Case 1: $i > j$

$$x_{i+1/2} - x_j = \frac{1}{2}h_j + (h_{j+1} + h_{j+2} + ... + h_i) = \frac{1}{2}h_j + \sum_{k=j+1}^{i} h_k$$

Then integral (A) becomes:

$$\int_{-h_j/2}^{h_j/2} \frac{z/\mu_j + 1}{\sqrt{|\frac{1}{2}h_j + \sum_{k=j+1}^{i} h_k - z|}} dz = \int_{-h_j/2}^{h_j/2} \frac{z/\mu_j + 1}{\sqrt{h_j}\sqrt{|\frac{1}{2} + \frac{1}{h_j}\sum_{k=j+1}^{i} h_k - \frac{z}{h_j}|}} dz.$$

Finally, let $w = z/h_j$, so that $z = h_j w$ and $dz = h_j dw$

$$\frac{h_j}{\sqrt{h_j}} \int_{-1/2}^{1/2} \frac{(h_j/\mu_j)w + 1}{\sqrt{\left|\frac{1}{2} - w + \frac{h_{j+1}+...+h_i}{h_j}\right|}} dw =$$

$$\sqrt{h_j} \int_{-1/2}^{1/2} \frac{(h_j/\mu_j)w + 1}{\sqrt{\left|\frac{1}{2} - w + (1/h_j)\sum_{k=j+1}^{i} h_k\right|}} dw. \tag{16}$$

Case 2: $i < j$

$$x_{i+1/2} - x_j = -\left(\frac{1}{2}h_j + (h_{i+1} + ... + h_{j-2} + h_{j-1})\right) = -\left(\frac{1}{2}h_j + \sum_{k=i+1}^{j-1} h_k\right)$$

The substitution is the same in this case, so integral (A) then is

$$\sqrt{h_j}\int_{-1/2}^{1/2} \frac{(h_j/\mu_j)w + 1}{\sqrt{\left|-\left(\frac{1}{2} + w + (1/h_j)\sum_{k=i+1}^{j-1} h_k\right)\right|}} dw. \tag{17}$$

Note that this is now over a unit interval.

Integral (B)

Let $z = y - x_{j+1}$, so that $y = z + x_{j+1}$ and $dz = dy$. The upper bound of the integral is $x_{j+3/2} - x_{j+1} = h_{j+1}/2$ and the lower bound is $x_{j+1/2} - x_{j+1} = -h_{j+1}/2$. The integral can be written as:

$$\int_{-h_{j+1}/2}^{h_{j+1}/2} \frac{(-1/\mu_{j+1})z}{\sqrt{\left|x_{i+1/2} - z - x_{j+1}\right|}} dz.$$

The issue again becomes the expression in the denominator–what is $x_{i+1/2} - x_j$?

Case 1: $i > j$

$$x_{i+1/2} - x_{j+1} = \frac{1}{2}h_{j+1} + (h_{j+2} + ... + h_i) = \frac{1}{2}h_{j+1} + \sum_{k=j+2}^{i} h_k$$

then integral (B) is:

$$\int_{-h_{j+1}/2}^{h_{j+1}/2} \frac{(-1/\mu_{j+1})z}{\sqrt{\left|\frac{1}{2}h_{j+1} - z + \sum_{k=j+2}^{i} h_k\right|}} dz.$$

If we let $w = z/h_{j+1}$ then our integral becomes:

$$\sqrt{h_{j+1}}\int_{-1/2}^{1/2} \frac{(-h_{j+1}/\mu_{j+1})w}{\sqrt{\left|\frac{1}{2} - w + (1/h_{j+1})\sum_{k=j+2}^{i} h_k\right|}} dw. \tag{18}$$

Case 2: $i < j$

$$x_{i+1/2} - x_{j+1} = -\left(\frac{1}{2}h_{j+1} + (h_j + h_{j-1} + ... + h_{i+1})\right) = -\left(\frac{1}{2}h_{j+1} + \sum_{k=i+1}^{j} h_k\right)$$

Using the same substitution, the integral (B) is:

$$\sqrt{h_{j+1}} \int_{-1/2}^{1/2} \frac{(-h_{j+1}/\mu_{j+1})w}{\sqrt{\left|-\left(\frac{1}{2} + w + (1/h_{j+1}) \sum_{k=i+1}^{j} h_k\right)\right|}} dw. \tag{19}$$

In summary, although the basis function integrals do not look quite as nice, we can still transform and shift them to be over a unit interval. Furthermore, if we let each $h_1 = \ldots = h_i = \ldots = h_N = h$, our integrals reduce to the same form as the uniform mesh case. Most importantly, however, we can still integrate them *exactly* and evaluate for the given values of the step sizes involved in the summations.

As in the uniform case, we can first test the correctness of these formulas by showing that linear reconstruction of linear data is exact, and in general, order n reconstruction of order n initial data is without error.

3.2 Nonuniform Linear Reconstruction Results

As mentioned, we expect that linear reconstruction of linear initial data should give exact answers. The following table confirms this expectation.

N	$\|\|error\|\|_\infty$	$rate_{L\infty}$	$\|\|error\|\|_1$	$rate_{L1}$
20	1.38777878078e-15	0.0588936890536	5.23747711867e-16	-0.133525454837
40	1.33226762955e-15	-0.415037499279	5.74536078435e-16	-0.118264873075
80	1.7763568394e-15	-0.807354922058	6.23617910783e-16	-0.500420557664
160	3.10862446895e-15	-0.893084796083	8.82186034293e-16	-0.420811399038
320	5.77315972805e-15	-0.206450877467	1.18096501409e-15	-0.419767384217
640	6.66133814775e-15	-0.793549122533	1.57979089236e-15	-0.515314498103
1280	1.15463194561e-14	-0.387023123109	2.2580041037e-15	-0.512348628603
2560	1.50990331349e-14		3.22075012503e-15	

Nonuniform Linear Upwind – Linear Data: $u(x, t = 0) = 3x - 2$

While useful, these results do not give us information about how quickly these results converge. The following cubic and wavepacket initial data, does however. The results are as follows.

N	$\|\|error\|\|_\infty$	$rate_{L\infty}$	$\|\|error\|\|_1$	$rate_{L1}$
20	0.0137179953324	2.33608989809	0.00128250962908	2.55453833821
40	0.00271679906349	2.40515353855	0.000218307154845	2.4285244792
80	0.000512901724862	2.44303754452	4.05517178182e-05	2.42022293174
160	9.43206050774e-05	2.46463183963	7.57616731996e-06	2.43800538938
320	1.70874975831e-05	2.47739793306	1.39809539651e-06	2.45564617839
640	3.0683675214e-06	2.48520480987	2.54867023662e-07	2.46891995504
1280	5.48007098367e-07	2.490125871	4.60356928643e-08	2.47828701797
2560	9.75401914793e-08		8.26144381546e-09	

Nonuniform Linear Upwind – Cubic Data: $u(x, t = 0) = 4x^3$

N	$\|\|error\|\|_\infty$	$rate_{L\infty}$	$\|\|error\|\|_1$	$rate_{L1}$
20	0.0779292654047	-0.119020694626	0.00434727906389	0.977351361032
40	0.0846309822798	2.04537796198	0.0022080324095	2.49042154904
80	0.0205026152841	2.88892245176	0.000392928794267	2.88744796719
160	0.00276794176962	2.9386872185	5.31013309504e-05	2.92577762188
320	0.000361013920842	2.80575322798	6.98809148111e-06	2.80619190709
640	5.16307063688e-05	2.66138192987	9.99103876607e-07	2.68068405633
1280	8.16116720909e-06		1.55827582902e-07	

Nonuniform Linear Upwind, $u(x, t = 0) = \cos^6(10\pi/3(x - 1/2)) \sin(50\pi/3(x - 1/2))$

And so we see that not only is the linear reconstruction method on nonuniform grids a stable method, but it also convergences at the same rate as its uniform counterpart, namely at $p \approx 2.5$.

3.3 Nonuniform Higher Order Reconstruction Results

Recalling the expressions in (15) for linear basis functions, we had

$$\varphi_j^{-1}(y) = \frac{-1}{\mu_j}(y - x_j) \qquad \varphi_j^0(y) = \frac{1}{\mu_j}(y - x_{j-1}) \tag{20}$$

where μ_j was simply the average of the step sizes in cells j and $j - 1$. These expressions did not change very much at all from their uniform grid counterparts. We merely replace $1/h$ with $1/\mu_j$. In general, however, the basis functions for higher order reconstructions are much more complicated. The expressions get to be extremely long and convoluted, resulting in a much heavier reliance on computer algebra systems than before. The implementation of the numerical method also required much more attention to detail than before. It is important to stress, however, that for each reconstruction method, whenever each of the nonconstant step values were replaced with a constant step size,

we recovered our original expressions from the uniform grid cases. This was always the first check of the accuracy of these formulas.

The following tables present one example of polynomial initial data and one of wavepacket initial data for both second and third order stencils. Again, we stress both the importance of stability and comparison of convergence rates.

N	$\|\|error\|\|_\infty$	$rate_{L\infty}$	$\|\|error\|\|_1$	$rate_{L1}$
20	0.000967392846719	3.33763828529	0.000127353447197	3.30061374312
40	9.56915596695e-05	3.40911135277	1.29248932294e-05	3.37057097922
80	9.0080099544e-06	3.44688475773	1.24963734905e-06	3.41911399842
160	8.26062968695e-07	3.46780153402	1.16822938154e-07	3.44925568401
320	7.46622155212e-08	3.479850717	1.06954411189e-08	3.46762554287
640	6.69208466419e-09	3.48703870684	9.66806138128e-10	3.4789400827
1280	5.96840354916e-10	3.49141304413	8.67109772854e-11	3.48615131814
2560	5.30686605771e-11		7.73816462469e-12	

Nonuniform Quadratic Upwind, $u(x, t = 0) = 4y^3$

N	$\|\|error\|\|_\infty$	$rate_{L\infty}$	$\|\|error\|\|_1$	$rate_{L1}$
20	0.188271972617	1.18440622651	0.00849492800548	1.6660583908
40	0.0828407213083	2.12261299376	0.00267686304656	2.79229618748
80	0.0190227671277	3.66471867129	0.000386421465478	3.73462639916
160	0.00149997301379	3.7311085541	2.90286389958e-05	3.77674752967
320	0.00011295562263	3.67826861404	2.11793380336e-06	3.68411474295
640	8.82345487344e-06	3.59231419053	1.64771971049e-07	3.59189756893
1280	7.31550554245e-07		1.3665150757e-08	

Nonuniform Quad. Upwind, $u(x, t = 0) = \cos^6(10\pi/3(x - 1/2)) \sin(50\pi/3(x - 1/2))$

N	$\|\|error\|\|_\infty$	$rate_{L\infty}$	$\|\|error\|\|_1$	$rate_{L1}$
20	0.000454058602189	3.39879802901	6.42590624472e-05	4.13404542083
40	4.30498608388e-05	3.4352112757	3.65984514291e-06	4.09415681163
80	3.97988127299e-06	3.45713469723	2.14288419881e-07	4.06260645852
160	3.62383882457e-07	3.47103490117	1.2824259513e-08	4.04643328724
320	3.26800906336e-08	3.48015100334	7.76130057666e-10	4.0331392883
640	2.92855517614e-09	3.48626120154	4.74065772554e-11	4.02403973362
1280	2.61326960072e-10	3.49042509743	2.91394893593e-12	4.02118145354
2560	2.32520669385e-11		1.79467453844e-13	

Nonuniform Quadratic Centered, $u(x, t = 0) = 4y^3$

N	$\|\|error\|\|_\infty$	$rate_{L\infty}$	$\|\|error\|\|_1$	$rate_{L1}$
20	0.101247505639	0.327343062307	0.00436319699339	1.09275530394
40	0.0806945589074	3.24513741124	0.0020457506457	3.32109519735
80	0.00851060729175	3.69963932139	0.000204693204065	3.97378669125
160	0.000655025401922	4.07497425227	1.30279005189e-05	4.08545142564
320	3.88658939031e-05	4.07014997753	7.67416281035e-07	4.10063220075
640	2.31382990984e-06	4.08197723763	4.4731938082e-08	4.08360312058
1280	1.36626153169e-07		2.63833953539e-09	

Nonuniform Quad. Centered, $u(x, t = 0) = \cos^6(10\pi/3(x - 1/2)) \sin(50\pi/3(x - 1/2))$

N	$\|\|error\|\|_\infty$	$rate_{L\infty}$	$\|\|error\|\|_1$	$rate_{L1}$
20	0.000626305009922	4.2808712459	5.44215471956e-05	5.01120108679
40	3.22192356395e-05	4.37425025124	1.6875204447e-06	4.79642002177
80	1.55358385356e-06	4.42503491006	6.0727128345e-08	4.54729232572
160	7.23213391396e-08	4.4537466697	2.59723565143e-09	4.44613673697
320	3.30031291185e-09	4.4705701236	1.19149118323e-10	4.43326759977
640	1.48860479499e-10	4.48123572679	5.51498463325e-12	4.43793491843
1280	6.66489086143e-12	4.51150033878	2.54444329918e-13	4.2381350958
2560	2.92210700081e-13		1.34830140759e-14	

Nonuniform Cubic Slight Upwind, $u(x, t = 0) = 6x^5 + 3x^2$

N	$\|\|error\|\|_\infty$	$rate_{L\infty}$	$\|\|error\|\|_1$	$rate_{L1}$
20	0.0845218867055	0.392837414923	0.00533374620757	1.53518945905
40	0.0643744212414	3.22322157145	0.0018403239195	3.81961472822
80	0.00689329654354	4.79866381902	0.0001303393845	4.63835561192
160	0.000247676734588	4.95208025675	5.2334911736e-06	4.97689723939
320	8.00129927964e-06	4.92472928322	1.66186653168e-07	4.9618509704
640	2.63432455627e-07	4.83780887239	5.33249142265e-09	4.85705464971
1280	9.21178294755e-09		1.83997120047e-10	

Nonuniform Cubic S.U., $u(x, t = 0) = \cos^6(10\pi/3(x - 1/2)) \sin(50\pi/3(x - 1/2))$

So, in general we observe both that the nonuniform versions of the numerical flux calculations are stable and that the rates of convergence are similar to their uniform counterparts.

4 Conclusion

We developed a computational model for efficiently solving the one way water equation and ultimately the full water wave equation. By framing the equation as a conservation law, we used polynomial approximations to our solution function based on cell averages in order to evaluate resulting flux integrals exactly. For uniformly spaced grids, we found that our rates of convergence were consistently a half-order higher than expected. For unevenly spaced grids, although the resulting analytic expressions are quite complicated, the rates of convergence are comparable to their uniform grid counterparts. Future computational work will be spent on time integration of the one way equation, and future theoretical work on finding the source of the extra half-order of convergence.

References

[1] Jennings, G.I., S. Karni, and J. Rauch. Absorbing Boundaries for the Water Wave Equation (in preparation). 2012.

[2] O. Runborg. Verifying Numerical Convergence Rates. pages 1–3, 2012.

[3] S. Wu. Well-posedness in Sobolev spaces of the full water wave problem in 2-D. 1997.